International Journal of Environmental Science and Technology (2023) 20:11997–12014
https://doi.org/10.1007/s13762-023-04931-8

ORIGINAL PAPER

Advanced oxidation processes for pharmaceutical degradation and disinfection of wastewater: peracetic acid and graphene oxide quantum dots

C. Tshangana[1] · M. P. Mubiayi[1] · A. Kuvarega[1] · B. Mamba[1] · A. Muleja[1]

Received: 15 September 2022 / Revised: 21 January 2023 / Accepted: 7 April 2023 / Published online: 29 April 2023

Abstract

A combination of graphene oxide quantum dots and peracetic acid (GQDs/PAA) was used to degrade sulfasalazine in municipal wastewater. The impact of reaction parameters such as initial concentrations of oxidant (peracetic acid) and drug (sulfasalazine) and different water matrices was evaluated. The degradation efficiency when using GQDs/PAA (50 mg/L: 0.10 mM) was almost 100% in synthetic water and 80% in municipal wastewater. The primary reactive radicals that caused the degradation of sulfasalazine in wastewater were identified as hydroxy (·OH) as well as the peroxy radicals ($CH_3C(=O)OO\cdot$, $CH_3C(=O)O\cdot$). 83.7% of total organic carbon were eliminated when 0.15 mM PAA was used while nearly 100% degradation of SZZ was achieved. A degradation pathway was proposed using the degradation intermediates obtained on quadrupole time-of-flight liquid chromatography mass spectrometry. The genotoxic and mutagenic potential of the degradation products formed during the degradation of sulfasalazine was assessed using the Ames test. It was demonstrated that none of the intermediates were mutagenic. GQDs/PAA was further tested as a potential disinfectant, and *S. aureus* was completely inactivated as verified by using LIVE/DEAD *Bac*light staining. In raw municipal wastewater, GQDs/PAA eliminated more than 90% of bacteria, thus confirming the synergy of GQDs/PAA as both a disinfectant and a photocatalyst.

Keywords Photocatalysis · Sulfasalazine · Bacterial viability · Degradation kinetics · Environmental remediation

Introduction

The prevalence and detection of residual pharmaceuticals and antibiotic-resistant bacteria (ARB) in effluents of wastewater treatment plants (WWTPs) are a global concern (Wang et al. 2020; Faleye et al. 2019). Most of the pharmaceuticals get excreted in their unmetabolized form either through urine or feces (Gašo-Sokač et al. 2017). Despite the low levels of pharmaceuticals detected in the environment, continued exposure poses substantial risks as their long-term effects in humans and animals remain unclear. Seasonal fluctuations also affect the frequency and concentrations of pharmaceuticals detected; the highest concentrations of pharmaceuticals are often detected during the winter season, and this is related to the increased utilization of medicine during winter when more people are prone to various illnesses (Wu et al. 2016).

The current study reports on a widely used class of pharmaceuticals known as sulfonamides which account for 16–21% of all antibiotic consumption annually (Göbel et al. 2005). Due to their extensive use, sulfonamides have been detected in surface water, secondary effluents and sludge (Paumelle et al. 2021; Ngigi et al. 2020; Raich-Montiu et al. 2007; Batt et al. 2007). For example, concentrations of sulfonamides varying from 7 to 88 µg/L have been reported (Wang et al. 2020). On the other hand, concentrations between 1.8 and 7.2 µM of sulfasalazine (SSZ) were reported to constitute significant threats to antimicrobial resistance. Additionally, the presence of sulfonamides can also increase antimicrobial resistance (Neafsey et al. 2010). Wang et al. (2020) reviewed the removal efficiencies of sulfonamides in full-scale treatment plants, and the finding showed that sulfonamides have a high propensity to resist biodegradation and generally exhibit a low removal

Editorial responsibility: Senthil Kumar Ponnusamy.

✉ A. Muleja
mulejaa@unisa.ac.za

[1] Institute for Nanotechnology and Water Sustainability, College of Science, Engineering and Technology, University of South Africa, Johannesburg 1709, South Africa

efficiency of 52.6%. Other sulfonamide removal efficiencies were reported in the ranges 38–74%, 33–75%, as well as 33% and 35%, respectively (Blair et al. 2015; Kasprzyk-Hordern et al. 2009; Snyder et al. 2007).

Most conventional processes in WWTPs were constructed more than 50 years. These WWTPs are ineffective in removing sulfonamides because they were not designed to deal with pharmaceutical contaminants. WWTPs were primarily designed to eliminate pollutants with chemical oxygen demand (COD) removal in the range 80–95% which is estimated to be 25% higher than most pharmaceuticals. As it stands, the removal efficiencies of antibiotics range between 40 and 70% and can be compared to the removal of total nitrogen in WWTPs (Qiu et al. 2010). The possibility of using disinfection (chlorination or UV) in the abatement of sulfanomides in WWTPs has been investigated previously. The reports revealed that after chlorination or UV treatment sulfamethoxazole concentrations were reduced to between 10 adn 70 ng/L and 20 and 40 ng/L, respectively (Yan et al. 2022). Although disinfection (chlorination and/or UV treatment) showed ability to treat sulfamethoxazole in the WWTPs, concerns relating to the generation of toxic disinfection by-products (DBPs) and the costly treatments cannot be ignored (Mazhar et al. 2020; Achour and Chabbi 2014). In addressing some of the limitations such as DBPs, researchers are suggesting the degradation of SSZ using advanced oxidative processes (AOPs). AOPs can be employed as an alternative standalone method or can be a hybrid complementing in existing water treatment procedures (Fan et al. 2011; Ji et al. 2018; Pelalak et al. 2020).

In AOPs, the highly reactive species generated via chemical and photochemical reactions are the main oxidants responsible for the degradation of contaminants. The most used peroxides in AOPs as sources of reactive radicals include persoxydisulfate (PDS), hydrogen peroxide (H_2O_2) and peroxymonosulfate (PMS). These peroxides were previously activated either by using transition metals, ultraviolet (UV) or by applying thermal treatment (Keyikoglu et al. 2020; Jazić et al. 2020; Chen et al. 2016). Peracetic acid (PAA; CH_3 C(O)OOH) is an organic peroxide that has great potential of producing similar highly reactive species (Chen et al. 2019). PAA has also been considered as a possible replacement for chlorine-based oxidants in the wastewater treatment largely because it does not generate toxic by-products during the disinfection process (Kitis 2004; Rossi et al. 2007).

In the current work, the use of a low-impact process that can simultaneously degrade pharmaceuticals and inactivate microorganisms using peracetic acid (PAA) activated by metal-free graphene oxide quantum dots (GQDs) is proposed. Unlike, in previously reported articles on the activation of PAA (Keyikoglu et al. 2020; Jazić et al. 2020; Chen et al. 2016), this study employs carbon-based nanomaterials and very little work has been openly published in this regard. The activation of PAA by GQDs typically generates free radicals [i.e., acetlyoxyl ($CH_3C(O)O\cdot$) and/or acetylperoxy $CH_3C(O)OO\cdot$] that are not prone to scavenging in complex water matrices by other possible ions (Tshangana et al. 2022; Cai et al. 2017; Rossi et al. 2007). Unlike chlorine, PAA exhibits disinfectant capabilities that are not dependent on pH, and it has been shown that PAA does not generate DBPs in the treated effluent (Kitis 2004). One of the core objectives of this work was therefore to determine and investigate the mutagenic potential of the reaction by-products of sulfasalazine degradation.

The main objectives of this study were to (a) investigate the degradation efficiency and kinetics of GQDs/PAA (keeping the concentration of GQDs constant while varying the concentrations of PAA) system against SSZ, (b) identify the main reactive radicals responsible for the degradation of SZZ, (c) investigate the mutagenic potential of the reaction by-products, (d) evaluate the effect of water matrices, initial concentration of SSZ and PAA dosage on SSZ degradation, (e) propose a photodegradation mechanistic pathway based on the detected reaction by-products determined by LC-Q-TOF-MS and finally (f) evaluate the inactivation of microbes in real wastewater and synthetic water with or without spiking the sample with *S. aureus* by GQDs/PAA. Further this study proposes the inactivation mechanism of GQDs/PAA by observing morphological changes on SEM and confirms the viability of the bacterial cells using the LIVE/DEAD cell viability test kit.

Materials and methods

Chemicals

Graphene oxide quantum dots suspension (1000 mg/L in H_2O), peracetic acid solution (36–40 wt% in acetic acid) and the chemicals used in determining reactive radical species (p-benzoquinone, 2,4-hexadiene, ethylenediaminetetraacetic acid disodium salt (EDTA-2Na), silver nitrate and methanol) were obtained from Sigma-Aldrich, South Africa. Sulfasalazine (Fig. 1), acetic acid, hydrogen peroxide, physiological saline solution, iodonitrotetrazolium chloride (INT), *Salmonella typhimurium* tester strains TA98 and TA100, nutrient broth, sodium thiosulfate, the 2,2 diphenyl-1-picrylhyrazyl (DPPH) glutaraldehyde, ascorbic acid and catalase were obtained from Merck, South Africa. The pH values of the solutions were adjusted using HCl or NaOH (0.1 and 0.01 M). All chemicals were used as received without further purification. Throughout the study, Milli-Q ultra-pure water was used, unless otherwise noted.

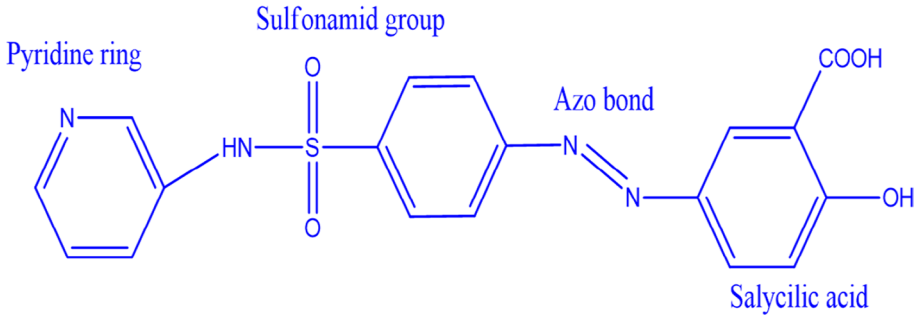

Fig. 1 Molecular structure of sulfasalazine ($C_{18}H_{14}N_{14}O_5S$)

Table 1 Water quality parameters of the collected wastewater

Properties	Values
pH	6.9 ± 0.25
Turbidity (NTU)	110 ± 3.26
Total organic carbon (TOC) (mg C/L)	22.30 ± 0.03
Electrical conductivity (µS/cm)	743 ± 5.31
Dissolved oxygen (DO) (mg/L)	10.9 ± 0.05

Sampling site and sample collection

The wastewater (WW) effluent sample was collected from a wastewater treatment plant in the Gauteng province (South Africa) and the water quality parameters (WQPs) are summarized in Table 1. Wastewater in this treatment plant passes through the following stages: (a) primary clarifier, (b) an aeration tank, (c) secondary clarifier and (d) through the disinfection process. For this study, the chosen sampling points were before the primary clarifier and after the secondary clarifier (labeled *sampling point 1* and *2*, respectively) as shown in the schematically in Scheme 1.

LC-QTOF-MS analysis

An Agilent 1200 binary pump system was used to perform LC-QTOF-MS analysis on an Acquity BEH C18 column (2.1 × 100 mm, 1.7 µm): the mobile phase (solvent A) (water containing 40 mM ammonium acetate with 2.5% acetonitrile at pH 7.8 adjusted with ammonia solution 2.5%) and solvent B (acetonitrile); after injection, isocratic conditions (100%) mobile phase A for 0.1 min and then linear gradient to 95% mobile phase over 2 min; followed by a gradient up to 55% mobile phase A in 8 min and isocratic conditions of 55% mobile phase A for a further 0.4 min before returning to 100% in 0.1 min; and followed by a reconditioning step at 100% mobile phase A for 5 min. The flow rate was 0.40 mL/min at 50 °C.

Detection conditions

Mass spectrometry (MS) tuning was conducted in negative electrospray ionization (ESI) mode. This was accomplished by employing a T-connector to infuse each analyte solution separately (concentration = 10 µg/mL), flow rate of 10 µL/

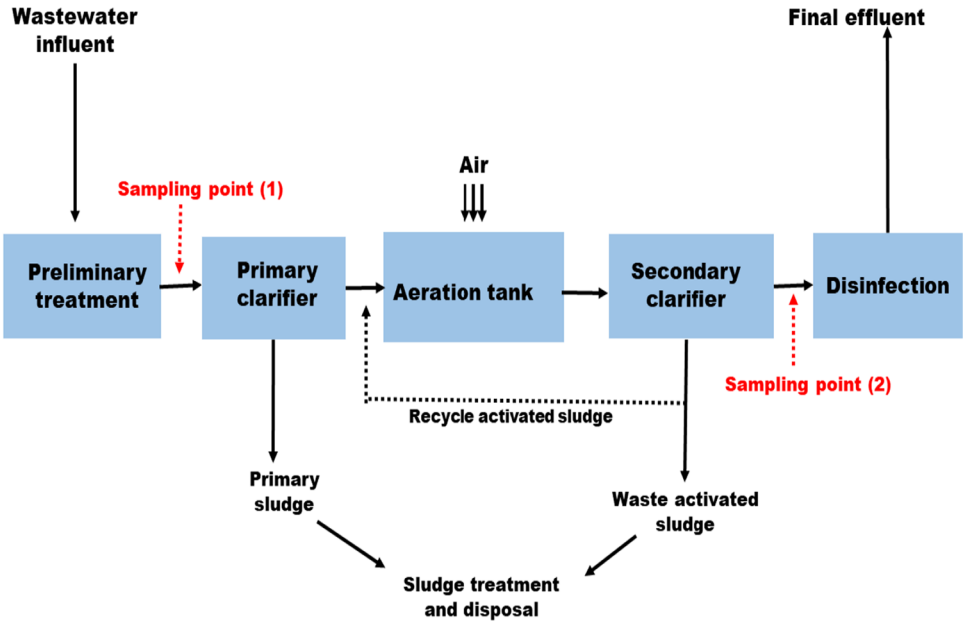

Scheme 1 Representation of the wastewater treatment plant where the samples were collected

min mixed with HPLC flow composed of solvent A and B (50: 50, *v/v*; 0.40 mL/min). Quantitative analysis was carried out using tandem MS in selected reaction monitoring (SRM) mode, alternating two or three transition reactions with varying dwell periods for each molecule.

Photodegradation of sulfasalazine (SSZ)

The degradation of SSZ experiments was performed at room temperature (20–22 °C) using a custom-made photoreactor from Lelesil Innovative Systems (India). A 250 W medium-pressure mercury vapor lamp of quartz bulb was used to irradiate light each aqueous sample solution where it was needed (Fig. 2). To determine the effect of initial SSZ concentration on the photodegradation process, three different concentrations of SSZ were used (200, 300 and 500 µM). The pH optimization studies were carried out, and the optimal pH value was 5. Other researchers (Omrania et al. 2019; Wu et al. 2019) have also reported pH 5 as ideal in the photodegradation of sulfasalazine and acetaminophen (Ghanbari et al. 2021). To this end, the pH of each of the SSZ solutions was maintained at pH 5 by adding (1:1) of 1 M HCl/NaOH. A set of experiments were conducted with real wastewater samples collected at the plant and with synthetic water from the laboratory. Both real wastewater and synthetic water samples (40 mL) were spiked with SSZ (10 mL; 10 ppm) to ensure detection with analytical instruments. For the photodegradation experiments, 150 mg/L of GQDs was added to the SSZ solution (10 ppm). The solutions (mixture of GQDs and SSZ) were initially mixed in the dark under stirring for 30 min, after which the UV–Vis light was turned on. The start of the reaction was timed shortly after adding the PAA at various concentrations (0.5, 1.0 and 1.5 mM). Aliquots (4 mL) were collected at 30-min intervals for 150 min and were immediately injected into a 1 mL phosphate buffer solution (0.20 mol/L, pH 8) to quench the reaction. The aliquots were further filtered through a 0.45 µm PVDF filter and analyzed using a UV–Vis spectrophotometer.

The absorbance of the filtrate was measured using a spectrophotometer to assess variations in SSZ concentrations under visible light irradiation. The percentage degradation of SSZ was calculated using Eq. 1.

$$\text{Sulfasalizine degradation } \% = \frac{(C_0 - C_t)}{C_0} \times 100\% \quad (1)$$

where C_0 and C_t represent the sulfasalazine concentration in the solution before and after irradiation, respectively.

The kinetic data (kinetic rate constants (k) and half-live ($t_{\frac{1}{2}}$)) of the photodegradation of SSZ were analyzed and calculated employing the integrated Langmuir–Hinshelwood (L–H) model Eq. 2 (Muleja and Mamba 2018):

$$\ln\left(\frac{C}{C_o}\right) = -k_1 t \quad (2)$$

where C and C_o are the concentration of SSZ after and before photodegradation experiments and k_1 is the pseudo-first-order rate constant. The determination of coefficient (R^2) values was used to determine goodnessof model fitness.

The half lifetimes were obtained using Eq. 3

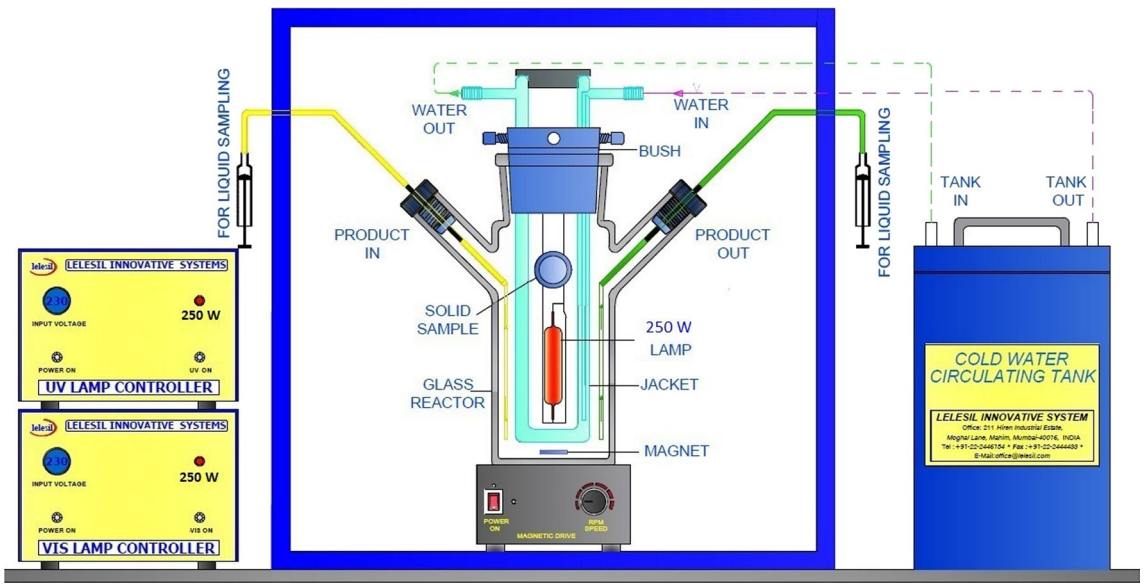

Fig. 2 Schematic representation of the photoreactor by Lelesil Innovative Systems used for the photodegradation of SSZ. Visible light mode of the reactor system was used in this study while the UV controller was turned off

$$t_{\frac{1}{2}} = \frac{0.693}{k'} \quad (3)$$

Radical species identification

The radical scavenging experiments were conducted similarly as detailed for the photodegradation experiments. The sole difference with previous experiments consisted of adding four radical scavengers at the beginning of each separate experiment. Silver nitrate, ethylenediaminetetra acetic acid diasoduim (EDTA-2Na), methanol and benzoquinone were used as scavengers at a concentration of 60 mM (Shafaee et al. 2018). In the case of acetyloxyl radicals, 4.0 mM of 2,4-hexadiene was used as a quencher (Li et al. 2021). Thereafter, the aliquots were filtered and analyzed using a UV–Vis spectrophotometer.

Determining mutagenic and genotoxic potential of possible reaction by-products from SSZ photodegradation using Ames test

The mutagenic and genotoxic potential of the reaction by-products formed during the SSZ degradation was tested using a *Salmonella* microsome assay as detailed by Mortelmans and Zeiger (2000). In the Ames assay, two *Salmonella typhirium* tester strains TA98 and TA100 without metabolic activation were used. 100 µL of the bacterial strains was incubated in Oxoid No.2 broth (20 mL) at 37 °C on a rotary shaker for 12 h. The cultured *Salmonella typhirium* tester strains (100 µL) were added to 100 µL of the aliquots collected at 0, 30, 60, 90, 120 and 150 min with 500 µL of phosphate buffer and top agar (2 mL) made up of biotin histidine (0.5 mM). From this, the top agar mixture was added to cover the surface of agar plate and incubated for 2 days at 37 °C. The positive and negative controls in the work were 2-nitroflurene for the TA98 and nitrofurantoin for T100.

Antimicrobial activity

Antimicrobial activity of a representative bacteria (*S. aureus*)

The model microbe used in this work was *S. aureus* (ATCC 25923); the efficiency of the antimicrobial activity of the GQDs/PAA system was tested against *S. aureus*. The experiments were conducted using the serial dilution method as reported by Elisha et al. (2017). Stock solutions of the GQDs, PAA and GQDs/PAA (1 mL) were used to serially dilute 96-well plates containing an overnight culture of *S. aureus*. The plates were incubated overnight at 37 °C and stained with iodonitrotetrazolium chloride (INT). All experiments were carried out in triplicates.

Antimicrobial activity in raw water

The experiments were similarly carried out as described for the photodegradation of SSZ with the difference that in this case SSZ solution was spiked with *S. aureus*. Another difference was that after quenching the PAA, 20 µL of the aliquots was collected at various intervals of time (0, 30, 60, 90, 120 and 150 min) and subsequently plated on nutrient agar (NA) plates. The nutrient agar plates were incubated at 37 °C, and the number of colonies were counted.

Scanning electron microscopy (SEM) analysis of *S. aureus*

S. aureus cells (logarithmic phase) were exposed to GQDs/PAA and irradiated using UV–Vis light for 10 min. The *S. aureus* cells were collected every 30 s and centrifuged at 5000 rpm for 3 min before being washed three times with sterile saline solution. The *S. aureus* cells were fixed overnight at 4 °C with glutaraldehyde and dehydrated with sequential treatment of 50%, 70%, 85%, 90% and 100% ethanol for 10 min each and gold sputter coated and observed using SEM instrument.

Cell viability using LIVE/DEAD *Bac*light staining kit

LIVE/DEAD *Bac*light staining kit was used to determine the viability of the *S. aureus* cells. The kit consisted of dyes, nucleic acid-binding SYTO® 9 and propidium iodide. SYTO® 9 can penetrate all bacterial membranes and stain green all *S. aureus* cells with intact cell membranes, while propidium iodide can only penetrate *S. aureus* cells with damaged membranes which are considered dead or to be dying. The viability tests were conducted as per manufacturer's guidelines, where 50 µL of SYTO® 9 and propidium iodide were mixed in a microfuge tube. 3 µL of this mixture was added to the GQDs/PAA treated with *S. aureus* suspension. The microfuge tubes were incubated for 30 min in the dark at room temperature. Following that, 5 µL of the stained *S. aureus* cells was pipetted onto a microscope slide, covered with a coverslip and imaged using a Zeiss laser scanning microscope LSM 780.

Results and discussion

Photodegradation of SSZ

Influence of PAA dosage on the photodegradation of SSZ

The dose of the oxidant was an important parameter in establishing whether GQDs/PAA system was an effective method for degrading SSZ. The effect of the dosage of

PAA on the photodegradation of SSZ was evaluated at pH 5 by varying the PAA concentration (0.05, 0.10 and 0.15 mM) while maintaining the GQDs concentration constant (50 mg/L). When 0.05 mM of PAA was added to the GQDs/PAA system, 80% of the drug was degraded after 150 min, while 99% and 99.8% of SZZ were degraded when using 0.10 and 0.15 mM of PAA, respectively (Fig. 3a). Increasing the PAA concentration resulted in almost complete degradation of the SSZ, implying that the trend observed (Fig. 3a) was dose-dependent. Interestingly, there was a negligible increment in the k_{obs} value from 0.036 to 0.038 min^{-1} at higher PAA concentrations. While the k_{obs} value increased at higher PAA concentrations, the growth rate remained almost the same which was ascribed to the PAA scavenging effect on the ·OH. Moreover, the phenomena were attributed to the limited reactive sites on GQDs available to accelerate the PAA activation in agreement with the literature (Chen et al. 2016). Another possibility is that the excessive PAA molecules can possibly absorb more photons which in turn inhibit the photodegradation of SSZ or the high loading of GQDs may produce too many reactive sites for PAA activation, quenching the reactive species produced by PAA activation (Zhang et al. 2020). Although the literature on the degradation of SZZ using PAA or GQDs is not readily available, Cai et al. (2017) investigated the UV/PAA on the degradation of seven pharmaceuticals and the results showed no significant degradation of the pharmaceuticals when using 1 mg/L (13.1 µM) of PAA at pH 7. When increasing the PAA dosage to 1 g/L and adding 0.11 g/L H_2O_2, Cai et al. (2017) reported 62.50% destruction for naproxen and 29.70% for diclofenac and the removal rate for the other pharmaceuticals was less than 11%. The degradation efficiencies of the GQDs/PAA in this study were all above 80% indicating improved removal efficiencies.

Effect of initial SSZ concentration

The initial concentration of SSZ was varied (10–50 mg/L) while maintaining the concentration of GQDs/PAA constant (50 mg/L: 0.10 mM) at pH 5 (Fig. 3b). From Fig. 3b, the lowest concentration of SSZ (10 mg/L) achieved the highest photodegradation efficiency of 100%, while the highest concentration of SSZ (50 mg/L) recorded the lowest removal efficiency of 20%. The degradation efficiency of SSZ was expected to decline with the increasing of the initial concentration of SSZ. The trend was observed in this study less catalytic sites when the concentration of SSZ was increased. Additionally, the decrease in the removal efficiency was also ascribed to less reactive species being available to degrade SSZ in agreement with previous finding (Santhosh et al. 2018). Gopinath and Krishna (2019) observed the same phenomenon when the initial concentration of 2, 4 dichlorophenol was increased during their experiment. In contrast, in this study at lower SSZ concentrations (10 and 20 mg/L) the number of catalytic sites was not a hindrance, and the rate of degradation was proportional to substrate concentration as per apparent first-order kinetics.

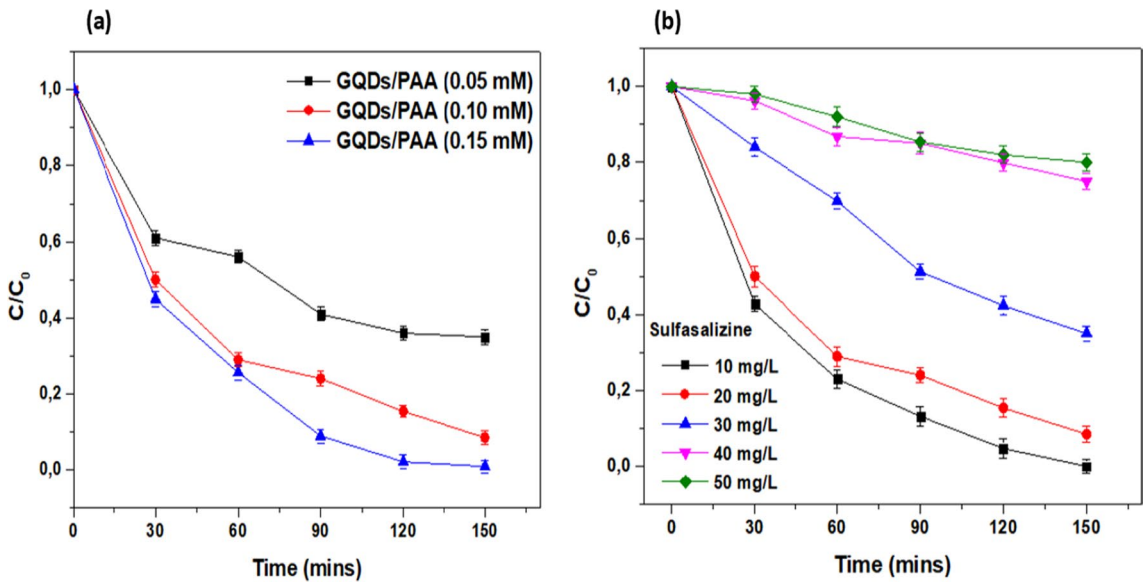

Fig. 3 **a** Influence of PAA dosage from 0.05 to 0.15 mM on the photodegradation of SSZ while keeping the concentration of the GQDs constant (50 mg/L: 0.10 mM) and pH 5; **b** influence of initial concentration of SSZ from 10 to 50 mg/L on the photodegradation process while keeping the concentration of the GQDs constant (0.05 g/L: 0.10 mM) and pH 5

Effect of water matrix

Real wastewater [collected at two sampling points at a South African wastewater treatment plant (Scheme 1)] and synthetic water were used as target matrices. The SSZ degradation profile in both water matrices is presented in Fig. 4a. In synthetic water using GQDs/PAA (50 mg/L: 0.10 mM), the obtained degradation efficiency was almost 100%, while 35% and 80% removal efficiency were recorded for wastewater collected at *sampling points 1* and *2*, respectively. The lower degradation efficiency of SSZ in wastewater compared to synthetic water was expected and it was largely ascribed to the complex nature of real wastewater. Numerous substances in real wastewater including humic acid, bicarbonates, chlorides and carbonates ions can scavenge radicals needed for the degradation of SSZ which in turn diminishes the degradation potential (Luo et al. 2015). The difference in degradation efficiencies of SSZ at the two sampling points was therefore due to the different composition of the water samples. In this WWTP, raw wastewater influent was pretreated prior to reaching *sampling point 1*. The only purpose of preliminary treatment was to screen coarse and large materials, remove the grit as well as to prevent organic solids from settling. Other researchers reported similar trends (Kirk et al. 2002). It has been demonstrated that approximately 50% of the incoming biochemical oxygen demand (BOD), 70% of the total suspended solids (TSS) and some organic nitrogen, phosphorous and heavy metals are only removed after the primary clarifier (Sonune and Ghate 2004). Sampling before the primary clarifier (*sampling point 1*) meant there were a lot of competition ions during the photodegradation process in the real wastewater. Luo et al. (2015)

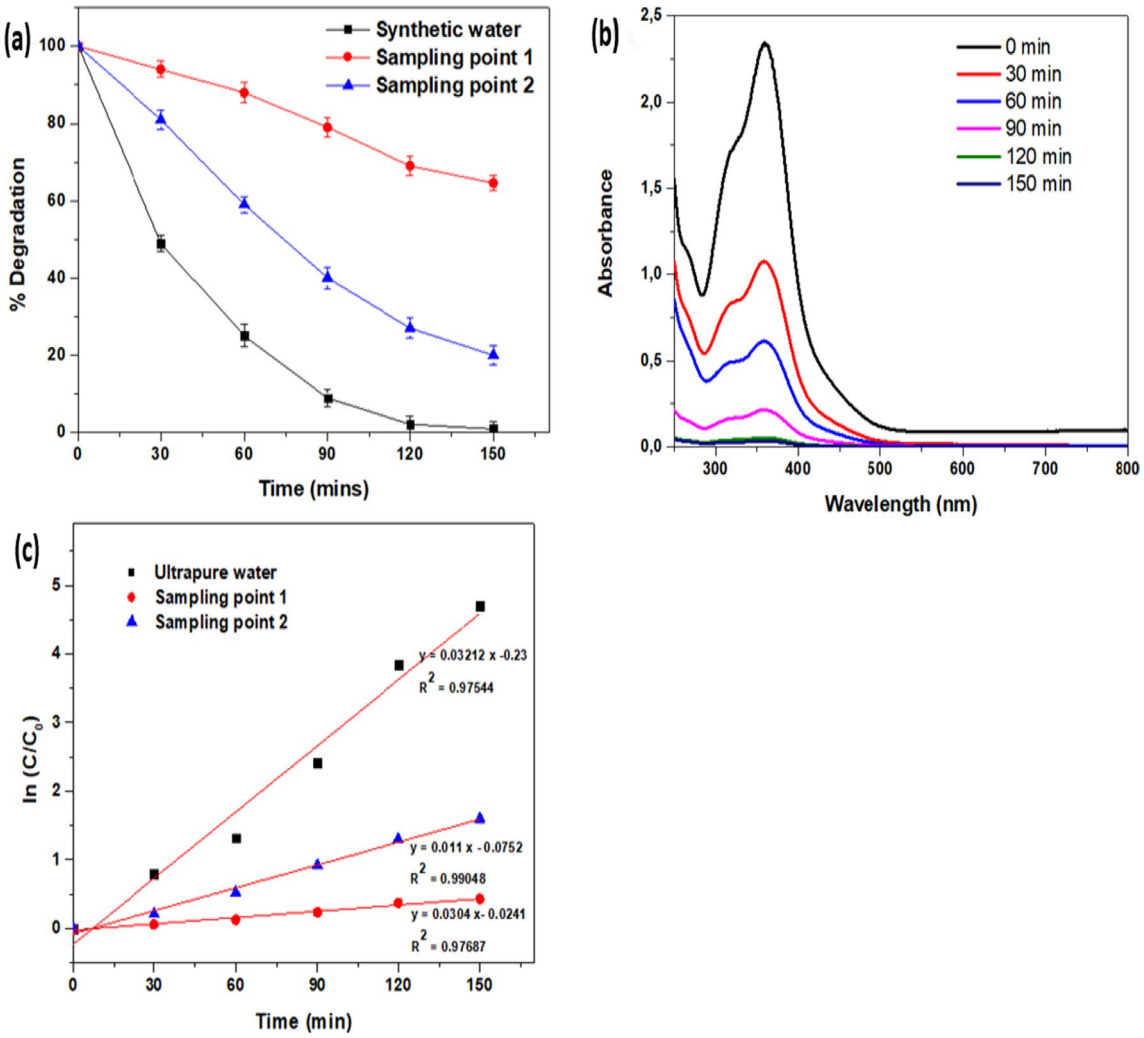

Fig. 4 **a** Photodegradation profile of SSZ in various water matrices while keeping the concentration of the GQDs constant (50 mg/L: 0.10 mM) at pH 5, **b** absorption spectra of SSZ during photodegradation process with increasing irradiation time from 0 to 150 min while keeping the GQDs concentration constant (50 mg/L: 0.10 mM) at pH 5 and **c** photodegradation kinetics of different water matrix when using PAA/GQDs system with constant GQDs parameters (50 mg/L: 0.10 mM) and pH 5

showed that carbonate and bicarbonate ions can affect the degradation process as they tend to react with ·OH and form CO_3·. In another instance, humic acid was shown to affect the degradation process either by acting as a scavenger or through the introduction of an inner filter effect arising from the large absorbance of humic acid (Shi et al. 2018). Cl^- ions can also affect the degradation process as they interact with ·OH and SO_4·$^-$ resulting in less reactive radicals such as ClOH·$^-$, Cl·, Cl^{2}·$^-$ (Kläning and Wolf 1985). At *sampling point 2* (after secondary clarifier), the effluent from the primary clarifier was treated using activated sludge to remove nitrogen, phosphorous, dissolved minerals as well as non-biodegradable organics similarly as reported in the literature (Sonune and Ghate 2004). The primary clarifier treatment implied that the water matrix was less complex and that most ions were removed and were not able to scavenge the radicals (responsible for photodegradation), hence the better degradation efficiency of 81% compared to the 35% at *sampling point 1*. In addition to efficiently degrading SSZ, the synergy of disinfection capabilities of GQDs/PAA was investigated using *S. aureus* as a representative bacterium in real wastewater (refer to "Antimicrobial activity of GQDs/PAA" section).

Photodegradation kinetics of SSZ

Variations in the absorption spectra of SZZ during the photodegradation are shown in Fig. 4b. Over time, the SSZ peak (wavelength 300–400 nm) decreased and eventually flattened out indicating complete degradation of SSZ. The data fit a pseudo-first-order model and a linear plot were obtained by plotting $\ln\left(\frac{C_0}{C}\right)$ versus irradiation time. The kinetic data of SSZ photodegradation in synthetic water and wastewater samples (*sampling point 1* and *2*) are presented in Fig. 4c. The linear relationship observed between the $\ln\left(\frac{C_0}{C}\right)$ over a period implied that first-order kinetics was followed in all samples. The synthetic water matrix had a higher rate constant (0.032 min^{-1}) compared to the wastewater samples (0.011 min^{-1} and 0.030 min^{-1}) for *sampling point 1* and *2*, respectively, and this can be explained by the complexity of the water matrix. Photodegradation efficiency and kinetic data for the degradation of SSZ are presented in Table 2. The degradation of SSZ in synthetic water was higher and showed shorter half-lives.

Identifying radicals responsible for the degradation of SSZ

The combination of GQDs and PAA degrades SSZ using a synergistic combination of different radicals to oxidize SSZ. The contribution of each radical was investigated by radical scavenging experiments, to identify the radicals responsible of the degradation of SSZ. Methanol, EDTA-2Na, benzoquinone and silver nitrate were used as scavengers for ·OH, h^+, ·O_2^- and e^-, respectively. To differentiate between the contribution of ·OH and the acetylperoxyl radicals, 2,4-hexadiene was used as a radical scavenger. The C=C double bonds of the 2,4-hexadiene can be readily attacked by the acetylperoxyl radicals, and it has been reported that 2,4-hexadiene can also react with ·OH at a reaction rate constant of 9.2×10 M^{-1} s^{-1}, meaning it quenches both ·OH and acetylperoxyl radicals (Zhang et al. 2020). SSZ was not affected by the addition of EDTA-2Na and silver nitrate, suggesting that h^+ and e^- had no active role in the photodegradation of SSZ (Fig. 5) and concurs with other previous studies (Wang et al. 2020; Cai et al. 2017). However, ·O_2^- was responsible for less than 8% of the active species. Methanol inhibited 43.9% of the ·OH radicals, indicating that ·OH contributed to the degradation of SSZ. The contribution of the ·OH was attributed to the presence of GQDs in the GQDs/PAA system. Recently, the contribution of ·OH in the degradation of two pharmaceuticals using the UV/PAA system has been highlighted (Cai et al. 2017). The contribution of ·OH occurs because of the molecular oxygen in the GQDs/PAA being reduced to ·O_2^-, and the resulting ·O_2^- will react with H^+ to form ·HO_2. The ·HO_2 will react with trapped e^- to produce H_2O_2. These H_2O_2 groups will interact with the generated conduction band e^- resulting in the production of more radicals. The presence of 2,4-hexadiene significantly inhibited the degradation of SSZ (76.4%), suggesting that the primary reactive species responsible for the photodegradation of SZZ were the acetylperoxyl (($CH_3C(O)O$·) or acetylperoxy $CH_3C(O)OO$·)) radicals. Other radicals such as ·CH_3, CH_3OO·, $CH_3C(=O)OO$· that were formed in the GQDs/PAA system had no impact on the photodegradation of SSZ, likely because since CH_3OO· is a weak peroxyl whose formation is dependent on the amount of O_2 present in the system. Additional tests were performed to rule out the potential of either acetic acid or H_2O_2 being involved in the photodegradation of SSZ. These tests employed the same amounts of acetic acid and H_2O_2 as the PAA solution (298.0 µM acetic acid and 86.0 µM H_2O_2 at 200.0 µM PAA). The results are depicted in Fig. 5b, c revealed that the contribution of both acetic acid and H_2O_2 was negligible in the degradation of SSZ. The above finding also confirmed that

Table 2 Photodegradation efficiency of SSZ degradation

Water matrix	Photodegradation (%)	Rate constant (min^{-1})	Half-life (min)	R^2
Synthetic water	99.99	0.032	21.57	0.975
Wastewater *Sampling point 1*	80.02	0.030	22.7	0.977
Wastewater *Sampling point 2*	34.62	0.011	63	0.990

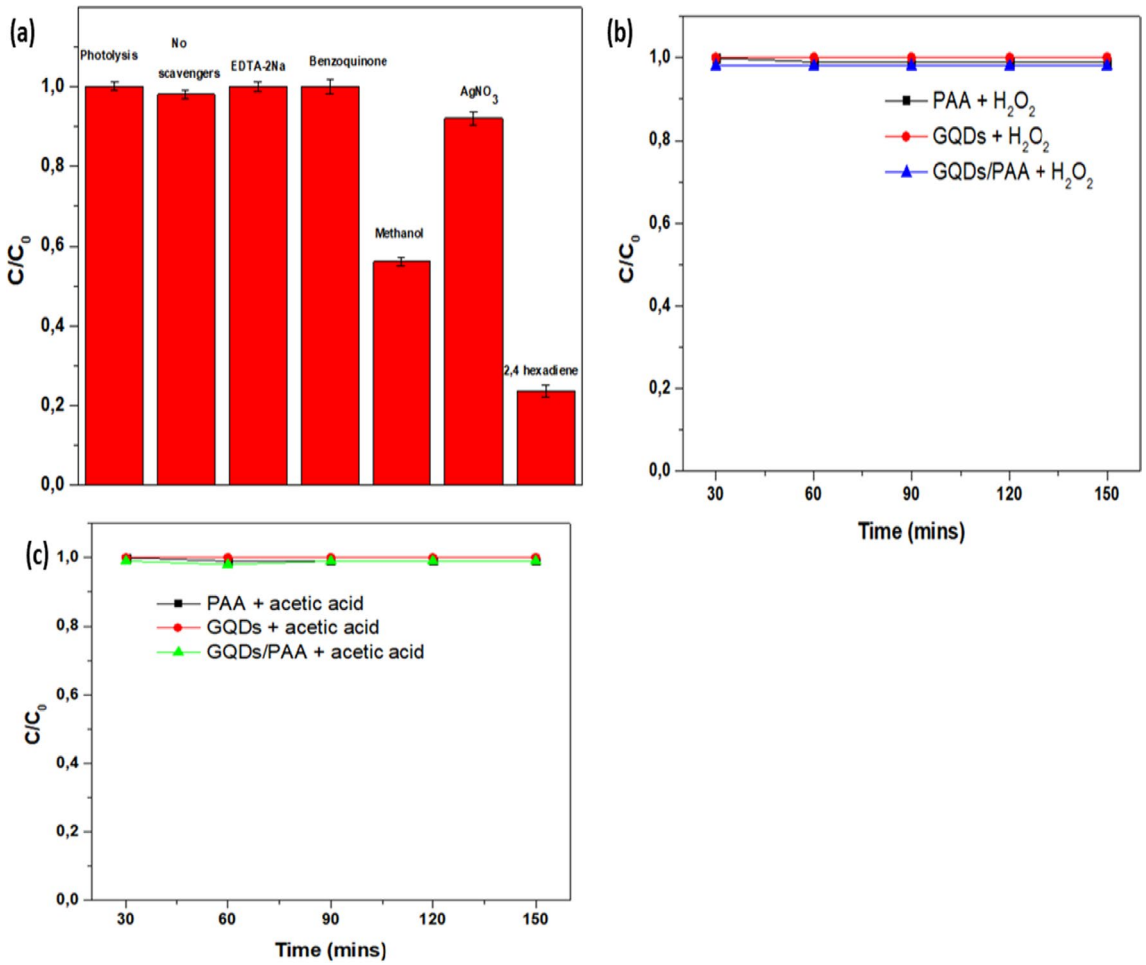

Fig. 5 **a** Radical scavenging experiments (For comparison purposes experiments in the dark and in the presence of light without scavengers are also included). **b** photodegradation of SSZ in the presence of H_2O_2 and **c** photodegradation of SSZ in acetic acid

GQDs were better suited to activate PAA compared to H_2O_2 owing to the peroxide bond energy of the PAA (159 kJ/mol) being less than H_2O_2 (213 kJ/mol). To support our argument, Wang et al. (2020) reported that the dissociation of the peroxide bond in PAA produces reactive species than H_2O_2.

The proposed radicals of PAA activated by GQDs in the degradation SZZ are shown in Eqs. 4–8. The rate-determining step and the homolysis of the oxygen–oxygen bond that is triggered by GQDs is represented by Eq. 4. CH_3· and CH_3O_2 (Eqs. 5, 6) were ruled out as contributors because CH_3· ($k = 2.8–4.1 \times 10^9$ M^{-1} s^{-1}) tends to quickly react with O_2 resulting in the formation of CH_3O_2. CH_3O_2 also has a significantly lower oxidation capacity (Cai et al. 2017); hence, the photodegradation of SSZ was likely due to ·OH, $CH_3C(=O)OO$· and $CH_3C(=O)O$·. The $CH_3C(O)OO$· radicals were reported to be stronger compared to the $CH_3C(O)O$· (Wang et al. 2020). Based on the latter, we propose various ways of the degradation of SSZ: (a) via the direct oxidation of SSZ consisting of the involvement of $CH_3C(O)O$· occurs via the direct reaction with SSZ or (b) indirectly when $CH_3C(O)O$· reacts with GQDs/PAA to form $CH_3C(O)OO$· which subsequently reacts with SSZ. The participation $CH_3C(O)O$· was informed by the cumulative effect of three reactions, namely the reaction of $CH_3C(O)O$· with SSZ, the direct reaction of $CH_3C(O)O$· with GQDs/PAA as well the self-decomposition of $CH_3C(O)O$·.

$$GQDs + CH_3C(=O)OOH \leftrightarrow GQDs + CH_3C(=O)O\cdot + \cdot OH \quad (4)$$

$$GQDs + CH_3C(=O)O\cdot \rightarrow CH_3\cdot + CO_2 \quad (5)$$

$$CH_3\cdot + O_2 \rightarrow CH_3O_2 \quad (6)$$

$$CH_3C(=O)OOH + \cdot OH \rightarrow CH_3C(=O)OO\cdot + H_2O \quad (7)$$

$$CH_3C(O)OOH + CH_3C(=O)O\cdot \rightarrow CH_3C(O)OO\cdot + CH_3C(O)OH \quad (8)$$

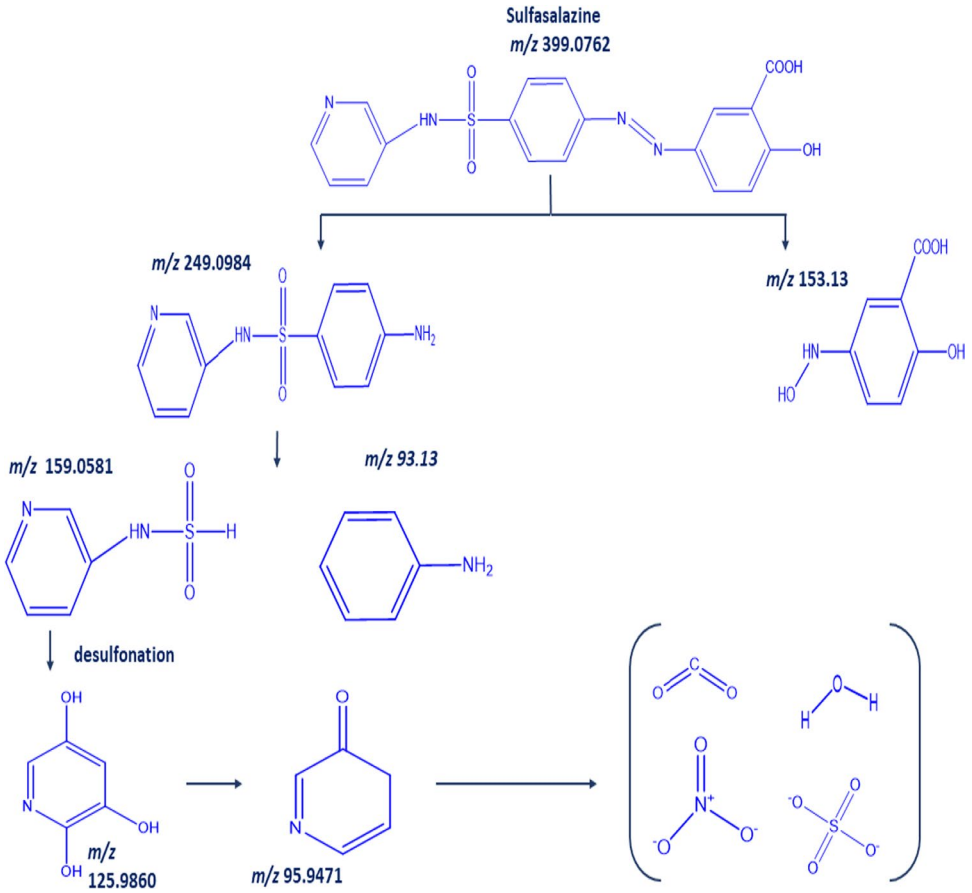

Scheme 2 Proposed transformation and photodegradation pathway of SSZ using GQDs/PAA

Proposed degradation pathway

The transformation and degradation pathway of SSZ with GQDs/PAA were evaluated using degradation products obtained using LC-QTOF-MS. Molecular ion masses and MS fragmentation patterns were employed to predict the molecular structure of the reaction intermediates. Typically, the chemical structure and functional moieties of SSZ allow it to be both oxidized and reduced during the photodegradation process. The oxidation process can occur as result of the –OH, –NH and –COOH of the SSZ attacking the OH, h^+ or $\cdot O_2^-$ radicals. Conversely, the –N=N– and –O=S=O bonds in SSZ facilitates its reduction (Omrania et al. 2019). From Scheme 2, ·OH and $CH_3C(=O)O\cdot$ attacked the –N=N– bonds of the parent molecule SSZ broke the SSZ in two intermediates, namely 5-aminosalysylic acid (*m/z* 153.13) and sulfapyridine (*m/z* 249.0984) (Fig. 6a, b). Other studies documented that further attack of the 5-aminosalysylic acid by either ·OH or h^+ ought to result in the intermediates 1,3,4-triol-2-carboxilic-1,3 dibutene and acetaldehyde or into maleic acid and ethandiol amine (Omrania et al. 2019); however, that was not the case in the present study. It is postulated that sulfapyridine was further attacked by the $CH_3C(=O)OO\cdot$ and the intermediate produced aniline (*m/z* 93.13) and (*m/z* 159.0581) (Fig. 6c, d). This intermediate underwent desulfonation and was further broken into pyridine 2,3,5-triol (*m/z* 125.9860) and pyridine-3(4H)-one (*m/z* 95.9471) (Fig. 6d). Although no smaller molecular masses were picked up on the LC-QTOF-MS, the resultant intermediates were able to undergo ring-opening caused by the reactive radicals ($CH_3C(=O)OO\cdot$). The latter formed lighter alcohols and acids which completely mineralized into CO_2 and H_2O.

Total organic carbon measurement

The TOC measurement graphs are presented in Fig. 7. TOC analysis showed 83.7% TOC eliminated when 0.15 mM PAA was used, even though there was an almost 100% degradation of SZZ. The incomplete TOC elimination was corroborated by LC-QTOF-MS results depicted in Fig. 6. This TOC elimination was attributed to the residual by-products that include aromatic ring structure of SSZ which was not completely by the GQDs/PAA. TOC showed that GQDs/PAA did not completely break the aromatic ring of SZZ within the reaction time into smaller molecules with low molecular weight such as CO_2 and H_2O. However, the residual by-products were less toxic and appeared in much lower

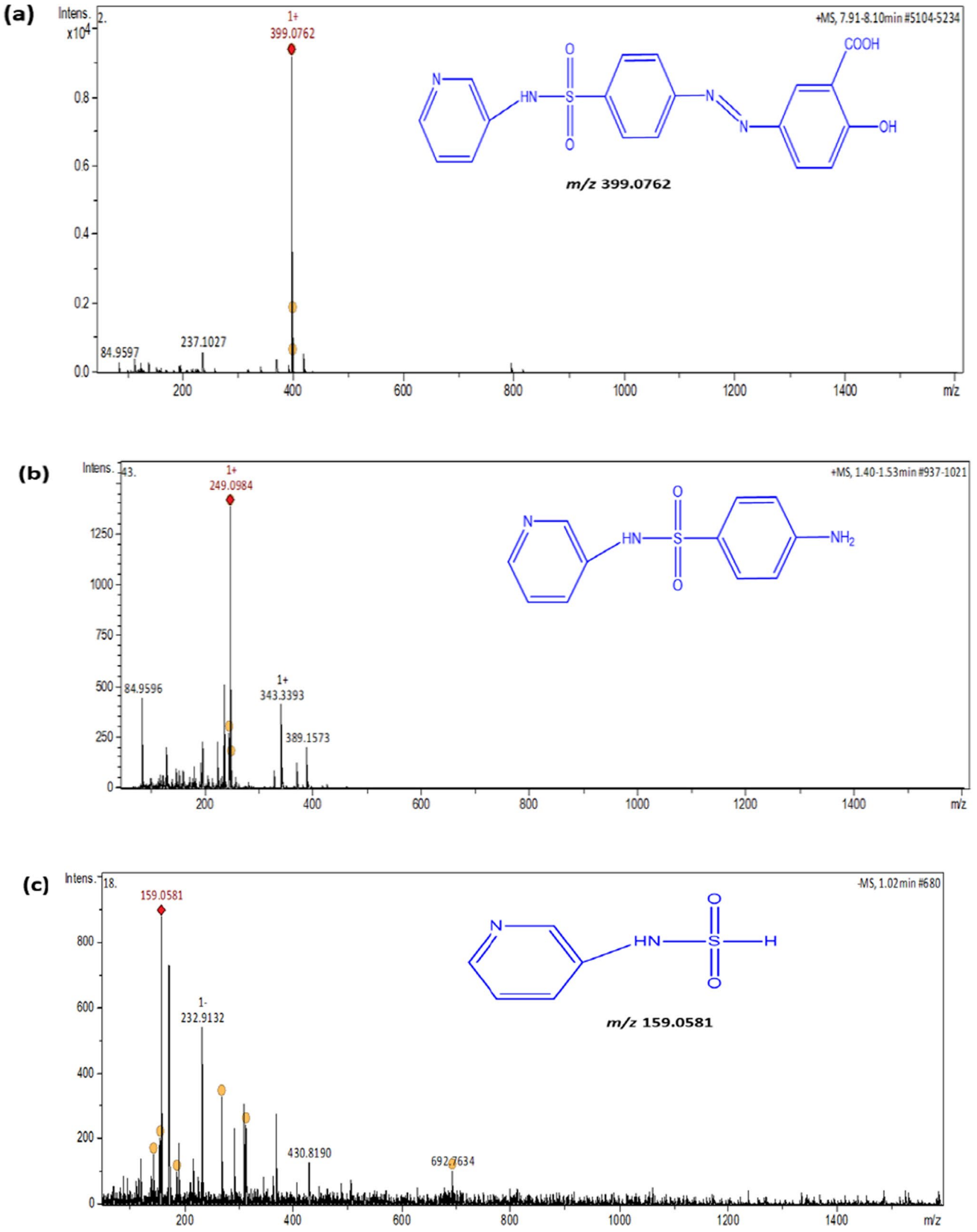

Fig. 6 LC-QTOF-MS degradation products of SSZ showing various steps of the pathway caused by the GQDs/PAA under visible light irradiation

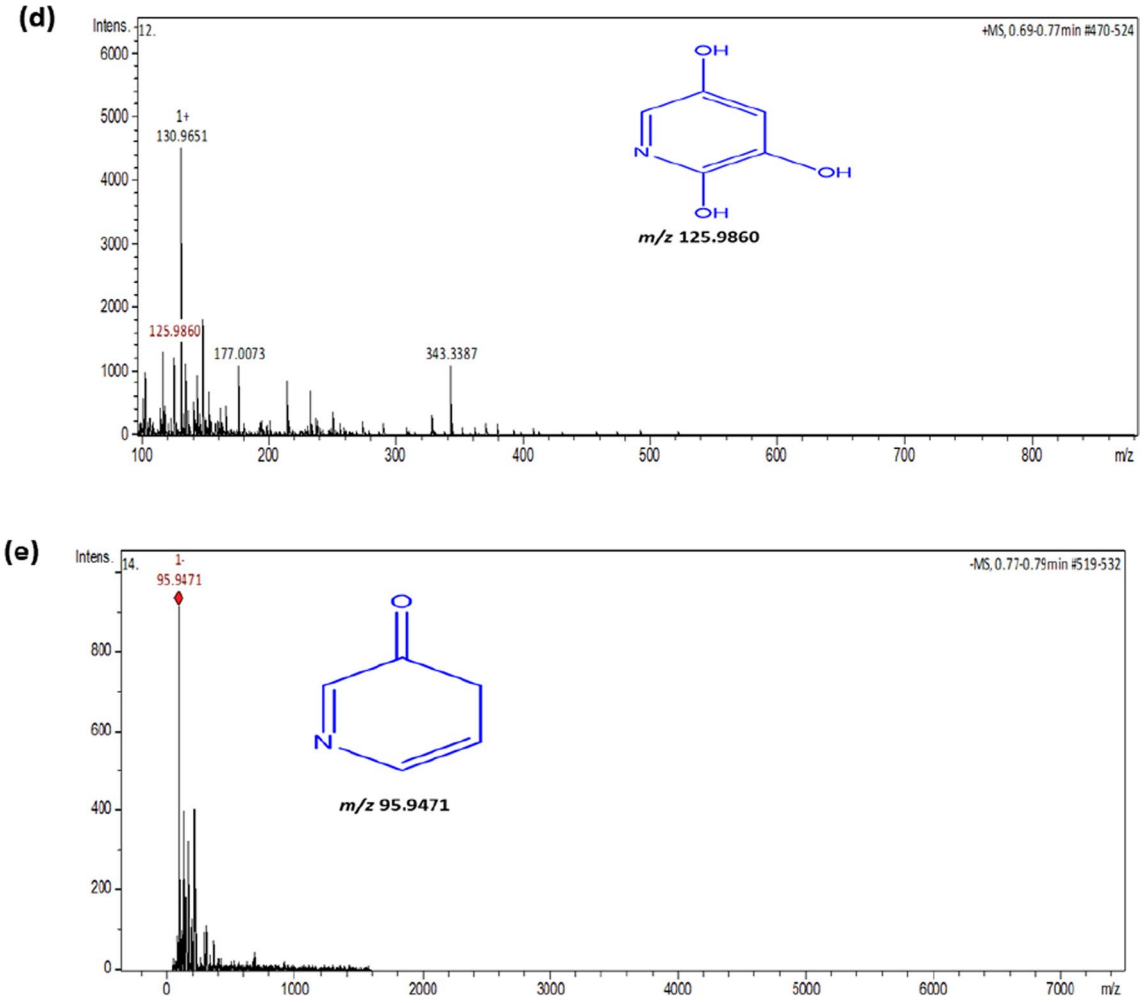

Fig. 6 (continued)

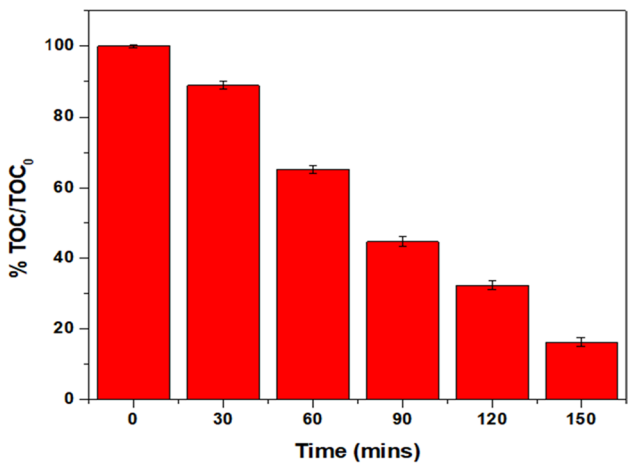

Fig. 7 TOC elimination of SSZ using GQDs/PAA

concentration than the parent pollutant. Additionally, PAA is an organic peroxide and has previously been reported to contribute partially to the TOC in the reaction (Zhang et al. 2020). Elsewhere, a low degree of mineralization of SSZ was observed when using Fenton-like processes, and in that case, however, the authors ascribed the 20% TOC elimination to the complexation of SSZ with Fe^{3+} (Fan et al. 2011). In this study, since SSZ was not completely mineralized, further tests were necessitated to evaluate the mutagenic and genotoxic potential of the reaction by-products formed during the degradation process.

Genotoxicity and mutagenicity test using Ames test

The TOC results (Fig. 7) indicate that some photodegradation intermediates remained in solution even after SSZ was completely degraded and that complete mineralization was not achieved. The trend corroborated to a report by Fan et al. (2011). To verify whether the reaction intermediates formed

during the photodegradation of SSZ were mutagenic, Ames assay was carried out. This assay, developed by Bruce Ames in 1970 (Ames et al. 1975) uses either *Salmonella* or *E. coli* bacterial strain to establish whether a specific chemical (in the case of this study the reaction by-products) are mutagenic. Typically, the bacterial strains used have a point mutation (histidine in *Salmonella typhimurium*) and (tryptophan in *E. coli)* that make it impossible for the bacterial strain to produce the corresponding amino acid. The point mutation results in the inability of the bacteria to produce corresponding amino acids and inhibit the growth of his- or trp-organisms unless histidine or tryptophan is supplied.

Culturing His-*Salmonella* in a medium containing the reaction by-products formed during the photodegradation of SSZ, may result in mutation on the histidine encoding gene, which allows *Salmonella* to regain the ability to synthesize histidine. If the reaction by-products formed during the degradation of SSZ cause this reversion, the by-products are considered as mutagens. The mutagenicity of the degradation by-products of SSZ are proportional to the number of bacterial colonies counted on the test plate. The assay was prepared using the aliquots collected at 30, 60, 90, 120 and 150 min. The genotoxicity was expressed as the % of micronuclei per 10.000 nuclei and presented as the average per dose ± SD (Table 3).

Results presented in Table 2 show that the reaction by-products are negative or weakly positive as per previous reports. The negative results give evidence that none of the reaction by-products were toxic. This agrees with previous reports on PAA forming less toxic or no by-products at all when used in the treatment of wastewater (Monarca et al. 2002a, b; Baldry 1988). Work reported by Monarca et al. (2002a, b) showed that no halogenated reaction by-products were formed after treating wastewater with PAA and mostly only carboxylic acids (which are not mutagenic) were found. While weakly positive results were observed at 90 and 120 min in the TA 100 strains, they were attributed to peroxy radicals and hydroxyl radicals formed during the synergy of GQDs/PAA. Li et al. (2012), Levin et al. (1982) and Dillon et al. (1998) found that the presence of superoxide, singlet oxygen, aldehydes gave positive results in the Ames assay. The reaction by-products from the SSZ degradation process did not induce any mutation in the two *Salmonella typhimurium* tester strains.

Table 3 Mutagenicity of reaction by-products in the photodegradation of SSZ using *Salmonella typhimurium* TA 98 and TA 100 tester strains

Reaction by-products/intermediates collected after	Number of colonies (mean ± SD)	
	TA 98	TA 100
0 min	16 ± 1	11 ± 1
30 min	14 ± 3	17 ± 1
60 min	11 ± 1	13 ± 2
90 min	14 ± 2	56 ± 6
120 min	16 ± 4	67 ± 8
150 min	11 ± 1	12 ± 2
Positive control	652 ± 28	722 ± 21

Antimicrobial activity of GQDs/PAA

Inactivation of representative bacteria *S. aureus*

The antimicrobial activity of the GQDs/PAA was evaluated on a representative bacterium, *S. aureus*. For comparative purposes the antimicrobial activity of PAA and GQDs was also evaluated. Results demonstrated that under the same experimental conditions both PAA and GQDs were able to inactivate *S. aureus*; however, the addition of PAA significantly enhanced the antimicrobial activity (Table 4). The minimum inhibitory concentration (MIC) is the concentration required to completely inhibit the growth of a microorganism. The lowest MIC was recorded for GQDs alone (45.1 µg/mL) and the highest recorded was for the GQDs/PAA (21.5 µg/mL). The improved antimicrobial activity of GQDs/PAA can be explained as follows: both GQDs and PAA have biocidal properties, the combined effect of GQDs/PAA led to complete cell destruction. The acetic acid of PAA is postulated to have reduced the intracellular pH as well as disrupted the chemiosmotic functions of the lipoprotein cytoplasmic membrane while the GQDs inactivate bacteria because of direct contact as well as the oxidation of cellular components (Hui et al. 2016; Baldry 1988). Chang et al. (2006) reported the MIC of *S. aureus* to be 0.33 mM when using 1 mM of PAA.

Bacterial inactivation mechanism of *S. aureus* and morphological observation by SEM

The mechanism of action of the GQDs/PAA against *S. aureus* was determined by morphological observation using SEM instrument. The inactivation process was tracked by monitoring changes in morphology of the cell wall and the cell membrane of the cellular materials in every SEM

Table 4 Minimum inhibitory concentration (µg/mL) of GQDs, PAA and GQDs/PAA

Materials	MIC concentrations (µg/mL) of *S. aureus*
GQDs	45.1
PAA	32.8
GQDs/PAA	21.5

micrograph. The SEM micrograph of the negative control (bacteria not exposed to GQDs/PAA) is shown in Fig. 8a; from this micrograph, an intact cell wall and the lining of the cellular material can be observed. The cell wall of the negative control is devoid of any artifacts and is relatively smooth. After 1 min of exposure to GQDs/PAA, the cell wall of the *S. aureus* started to disintegrate. It can be postulated that the PAA initially diffused through the cell wall of *S. aureus,* resulting in changes in the morphology of the cell wall. The cell wall visibly looks thinner and appears to erode at the surface and has a rougher edge, the same can be said about the cellular contents after 1 min (Fig. 8b). After the diffusion of the PAA into the *S. aureus* cell wall, the GQDs easily attach to the phospholipid lipid bilayer due to the electrostatic interactions resulting in further roughening of the cell wall and this is accompanied by an apparent deformation of the cellular material (Fig. 8c). Once inside the cell, GQDs accumulate in the nucleus and the oxidative radicals inhibit adenosine triphosphate (ATP), the replication of cells as well as cell respiration. Further exposure to GQDs/PAA (Fig. 8d, e) resulted in the complete destruction of the cell cortex and DNA compression. After 5 min, the *S. aureus* cells were destroyed and reduced to microscopic debris (Fig. 8f). Based on the SEM micrographs, it can be postulated that no regrowth of bacterial cells occur due to the damage on the *S. aureus* being irreparable.

Cell viability

To further confirm the antimicrobial activity of the GQDs/PAA on *S. aureus*, LIVE/DEAD *Bac*Light staining kit was used. Live healthy *S. aureus* cells (negative control) before GQDs/PAA treatment were green in color (Fig. 9). A1 min after GQDs/PAA treatment, both red and green stains were seen in the photomicrograph, suggesting that some *S. aureus* cells were beginning to die. The observed changes in the integrity of *S. aureus* cell membrane integrity are due to the combined effect of GQDs/PAA in denaturing proteins and oxidizing enzymes which results in impaired intracellular cellular solute levels. After 3 min, a complete inactivation of *S. aureus* cells was marked by all the *S. aureus* staining red. These photomicrographs verified the role that GQDs/PAA in the loss of cell membrane integrity of *S. aureus.* Using the same staining kit, results obtained by Costa et al. (2015)

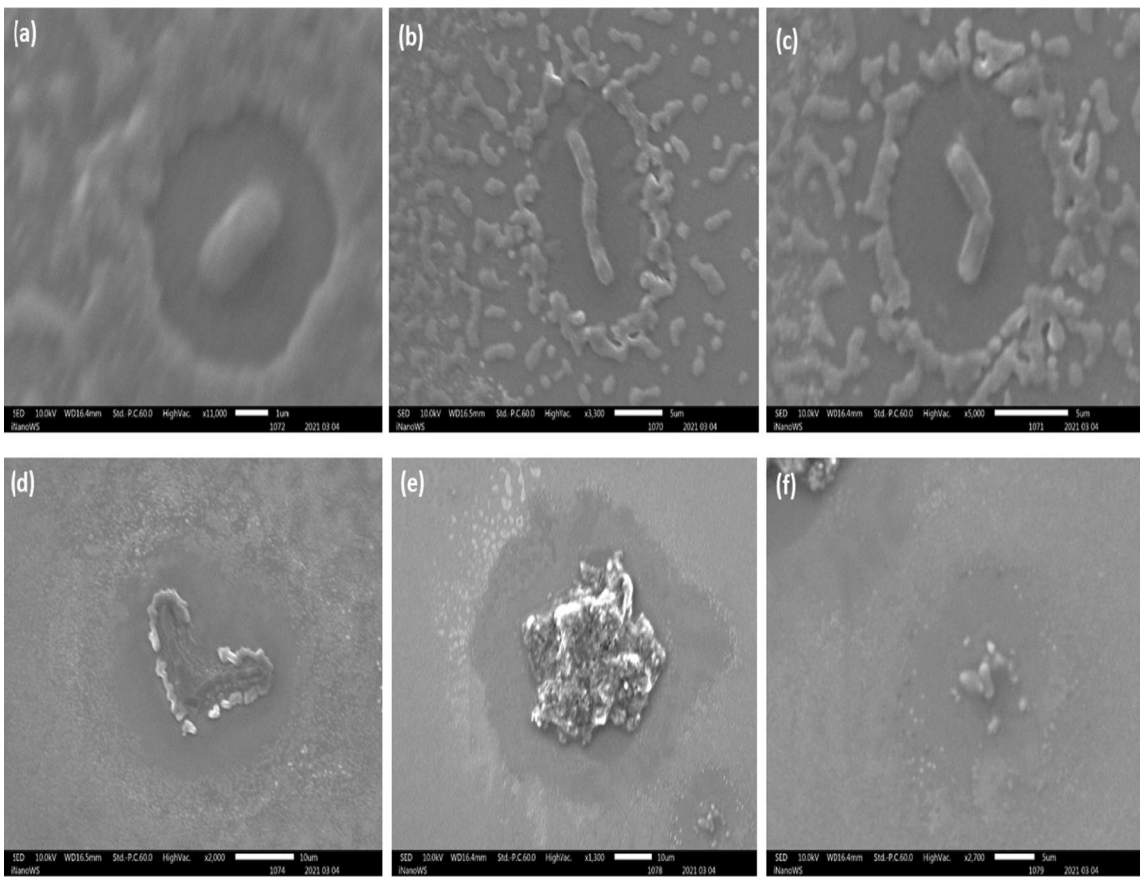

Fig. 8 SEM micrographs of **a** *S. aureus* cells without GQDs/PAA (control), *S. aureus* cells after GQDs/PAA treatment for **b** 1 min, **c** 2 min, **d** 3 min, **e** 4 and **f** 5 min under irradiation

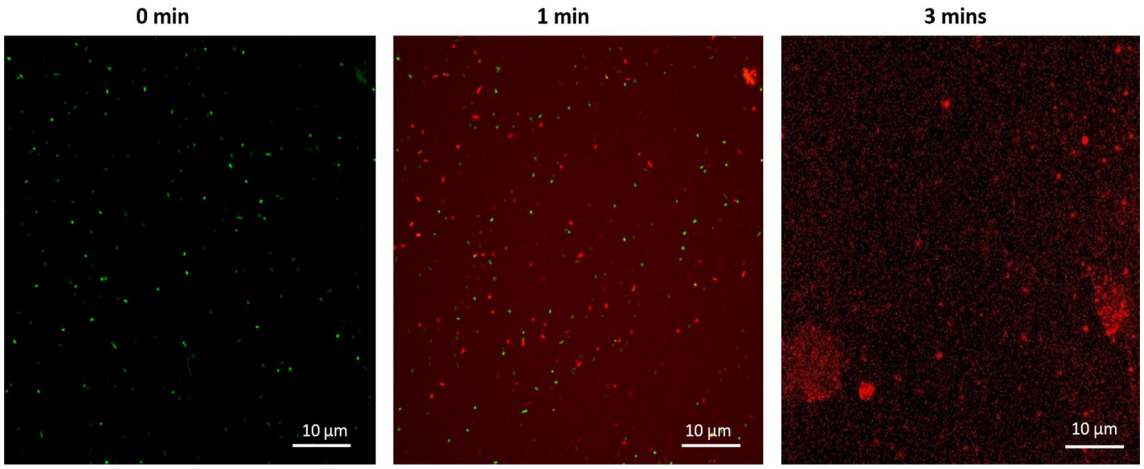

Fig. 9 Photomicrographs of *S. aureus* cells without GQDs/PAA and after GQDs/PAA treatment after 1 and 3 min

found that 2% and 0.25% of PAA were able to inactivate *S. aureus* after 30 min contact time, while elsewhere (Lee et al. 2016) obtained 100% inactivation of *S. aureus* on a biofilm after 60 s.

Antimicrobial activity in real wastewater without spiking with model *S. aureus*

To examine the feasibility of the GQDs/PAA to be use as a disinfectant, the disinfection ability was tested in raw wastewater collected at *sampling point 1 and 2* (Scheme 1). The GQDs/PAA was added to WW samples under irradiation (experiments carried out as detailed in "Photodegradation of sulfasalazine (SSZ)" section) except using raw wastewater and no addition of SSZ. (Only GQDs/PAA was used.) The aliquots were collected at 30-min intervals and immediately mixed with 200 µL of sodium thiosulfate and 500 µL catalase to stop the PAA from reacting further. A total of 20 µl of the solution was spread-plated and incubated at 37 °C for 24 h.

Figure 10 shows the microbial plate count, at time = 0 (before treatment with GQDs/PAA) and a significant number of colonies were observed on the plate. Increasing the exposure time to GQDs/PAA led to reduced number of colonies on the plate. After 150 min, only 9 colonies were present, indicating that the synergistic effect of the combination of GQDs and PAA was able to inactivate microbial species even in complex water matrices. Further studies need to be carried out to correctly identify the bacterial species that were not inactivated by GQDs/PAA. In an earlier study, Lefevre et al. (1992), Liberti and Notarnicola (1999) cited that the limitation of PAA being used as a disinfectant was in its inability of inactivating viruses and protozoa at reasonable doses. More recently, Mezzanotte et al. (2003) have showed that PAA efficacy was limited to other bacteria at lower doses. The recommendation from the study would be to vary the doses of PAA, the photocatalyst and even the contact time to yield better results.

Conclusion

The combination of graphene oxide quantum and peracetic acid (GQDs/PAA) was used to photodegrade sulfasalazine in municipality wastewater. A dose-dependent trend was observed wherein increasing the PAA concentration resulted in almost complete photodegradation of the SSZ. The degradation was accompanied by an increment in the k_{obs} value at higher PAA concentrations. Increasing the initial concentration of SSZ (10–50 mg/L) at a constant concentration of GQDs/PAA (50 mg/L: 0.10 mM) resulted in 10 mg/L of SSZ yielding the highest photodegradation efficiency of 100%; in contrast, the highest concentration of SSZ (50 mg/L) recorded the lowest removal efficiency of 20%. The primary reactive radicals in the photodegradation were hydroxy (·OH) as well as peroxy radicals $CH_3C(=O)OO·$ and $CH_3C(=O)O·$. Furthermore, the genotoxic and mutagenic potential of the degradation products formed during the degradation of sulfasalazine was non-mutagenic. GQDs/PAA completely inactivated *S. aureus* and eliminated more than 90% of bacteria present in raw municipal wastewater. This contribution presents an opportunity to simultaneously degrade pharmaceuticals and their active metabolites as well as inactivate microorganisms using GQDs/PAA. The results indicate practical application in real wastewater treatment plant where PAA-based GQDs advanced oxidation processes could be utilized in the tertiary stage of a wastewater reclamation treatment facility for water reuse and environmental remediation.

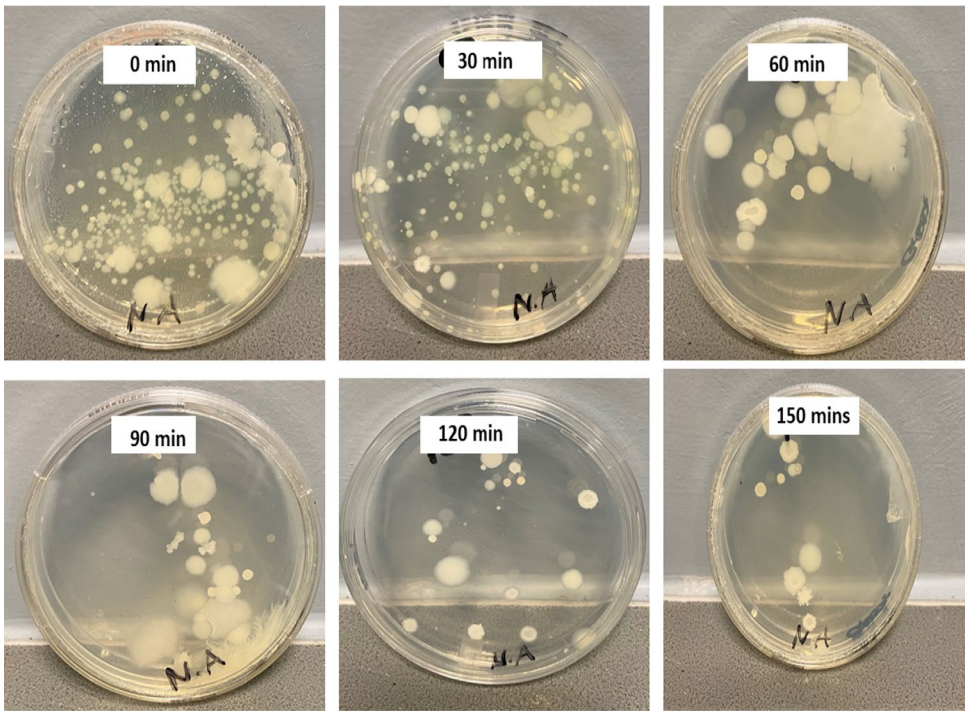

Fig. 10 Bacterial colonies formed after treating raw wastewater with GQDs/PAA after 150 min

Acknowledgements The authors gratefully acknowledge funding from the Institute for Nanotechnology and Water Sustainability (iNanoWS) at the College of Science, Engineering and Technology (CSET), University of South Africa.

Author contributions CT was involved in conceptualization, investigation, methodology, formal analysis and writing—original draft preparation. MPM was responsible for writing—reviewing and editing. AK contributed to methodology, investigation and writing—reviewing and editing. BM took part in supervision, resources, writing—reviewing and editing. AM participated in supervision, investigation, methodology, writing—reviewing and editing.

Funding Open access funding provided by University of South Africa.

Declarations

Conflict of interest The authors declare that they have no known competing financial interests or personal relationships that could have appeared to influence the work reported in this paper.

References

Achour S, Chabbi F (2014) Disinfection of drinking water-constraints and optimization perspectives in Algeria. LARHYSS Journal P-ISSN 1112-3680/E-ISSN 2521-9782

Ames BN, McCann J, Yamasaki E (1975) Methods for detecting carcinogens and mutagens with the Salmonella/mammalian-microsome mutagenicity test. Mutat Res 31(6):347–363

Baldry MGC (1988) Disinfection with peroxygens. Ind Biocides Crit Rep Appl Chem. 23:91–116

Batt AL, Kim S, Aga DS (2007) Comparison of the occurrence of antibiotics in four full-scale wastewater treatment plants with varying designs and operations. Chemosphere 68(3):428–435. https://doi.org/10.1016/j.chemosphere.2007.01.008

Blair B, Nikolaus A, Hedman C, Klaper R, Grundl T (2015) Evaluating the degradation, sorption, and negative mass balances of pharmaceuticals and personal care products during wastewater treatment. Chemosphere 134:395–401. https://doi.org/10.1016/j.chemosphere.2015.04.078

Cai M, Sun P, Zhang L, Huang CH (2017) UV/peracetic acid for degradation of pharmaceuticals and reactive species evaluation. Environ Sci Technol 51(24):14217–14224. https://doi.org/10.1021/acs.est.7b04694

Chang W, Toghrol F, Bentley WE (2006) Toxicogenomic response of *Staphylococcus aureus* to peracetic acid. Environ Sci Technol 40(16):5124–5131. https://doi.org/10.1021/es060354b

Chen J, Zhang L, Huang T, Li W, Wang Y, Wang Z (2016) Decolorization of azo dye by peroxymonosulfate activated by carbon nanotube: radical versus non-radical mechanism. J Hazard Mater 320:571–580. https://doi.org/10.1016/j.jhazmat.2016.07.038

Chen S, Cai M, Liu Y, Zhang L, Feng L (2019) Effects of water matrices on the degradation of naproxen by reactive radicals in the UV/peracetic acid process. Water Res 150:153–161. https://doi.org/10.1016/j.watres.2018.11.044

Costa SADS, Paula OFPD, Silva CRG, Leão MVP, Santos SSFD (2015) Stability of antimicrobial activity of peracetic acid

solutions used in the final disinfection process. Braz Oral Res 29:1–6. https://doi.org/10.1590/1807-3107BOR-2015.vol29.0038

Dillon D, Combes R, Zeiger E (1998) The effectiveness of Salmonella strains TA100, TA102 and TA104 for detecting mutagenicity of some aldehydes and peroxides. Mutagenesis 13(1):19–26. https://doi.org/10.1093/mutage/13.1.19

Elisha IL, Botha FS, McGaw LJ, Eloff JN (2017) The antibacterial activity of extracts of nine plant species with good activity against *Escherichia coli* against five other bacteria and cytotoxicity of extracts. BMC Complement Altern Med 17(1):1–10. https://doi.org/10.1186/s12906-017-1645-z

Faleye AC, Adegoke AA, Ramluckan K, Fick J, Bux F, Stenström TA (2019) Concentration and reduction of antibiotic residues in selected wastewater treatment plants and receiving waterbodies in Durban, South Africa. Sci Total Environ 678:10–20. https://doi.org/10.1016/j.scitotenv.2019.04.410

Fan X, Hao H, Shen X, Chen F, Zhang J (2011) Removal and degradation pathway study of sulfasalazine with Fenton-like reaction. J Hazard Mater 190:493–500. https://doi.org/10.1016/j.jhazmat.2011.03.069

Gašo-Sokač D, Habuda-Stanić M, Bušić V, Zobundžija D (2017) Occurrence of pharmaceuticals in surface water. Croat. J Food Sci Technol 9(2):204–210. https://doi.org/10.17508/CJFST.2017.9.2.18

Ghanbari F, Giannakis S, Lin KYA, Wu J, Madihi-Bidgoli S (2021) Acetaminophen degradation by a synergistic peracetic acid/UVC-LED/Fe (II) advanced oxidation process: kinetic assessment, process feasibility and mechanistic considerations. Chemosphere 263:128119. https://doi.org/10.1016/j.chemosphere.2020.128119

Göbel A, Thomsen A, McArdell CS, Alder AC, Giger W, Theiß N, Löffler D, Ternes TA (2005) Extraction and determination of sulfonamides, macrolides, and trimethoprim in sewage sludge. J Chromatogr A 1085(2):179–189

Gopinath A, Krishna K (2019) Photocatalytic degradation of a chlorinated organic chemical using activated carbon fiber coupled with semiconductor. Photochem Photobiol 95(6):1311–1319. https://doi.org/10.1111/php.13130

Hui L, Huang J, Chen G, Zhu Y, Yang L (2016) Antibacterial property of graphene quantum dots (both source material and bacterial shape matter). ACS Appl Mater Interfaces 8(1):20–25. https://doi.org/10.1021/acsami.5b10132

Jazić JM, Đurkić T, Bašić B, Watson M, Apostolović T, Tubić A, Agbaba J (2020) Degradation of a chloroacetanilide herbicide in natural waters using UV activated hydrogen peroxide, persulfate and peroxymonosulfate processes. Environ Sci Water Res Technol 6:2800–2815. https://doi.org/10.1039/D0EW00358A

Ji Y, Yang Y, Zhou L, Wang L, Lu J, Ferronato C, Chovelon JM (2018) Photodegradation of sulfasalazine and its human metabolites in water by UV and UV/peroxydisulfate processes. Water Res 133:299–309. https://doi.org/10.1016/j.watres.2018.01.047

Kasprzyk-Hordern B, Dinsdale RM, Guwy AJ (2009) The removal of pharmaceuticals, personal care products, endocrine disruptors and illicit drugs during wastewater treatment and its impact on the quality of receiving waters. Water Res 43(2):363–380. https://doi.org/10.1016/j.watres.2008.10.047

Keyikoglu R, Karatas O, Khataee A, Kobya M, Can OT, Soltani RDC, Isleyen M (2020) Peroxydisulfate activation by in-situ synthesized Fe_3O_4 nanoparticles for degradation of atrazine: performance and mechanism. Sep Purif Technol 247:116925. https://doi.org/10.1016/j.seppur.2020.116925

Kirk LA, Tyler CR, Lye CM, Sumpter JP (2002) Changes in estrogenic and androgenic activities at different stages of treatment in wastewater treatment works. Environ Toxicol Chem Int J 21(5):972–979. https://doi.org/10.1002/etc.5620210511

Kitis M (2004) Disinfection of wastewater with peracetic acid: a review. Environ Int 30:47–55. https://doi.org/10.1016/S0160-4120(03)00147-8

Kläning UK, Wolff T (1985) Laser flash photolysis of HClO, ClO−, HBrO, and BrO− in aqueous solution. Reactions of Cl-and Br-atoms. Ber Bunsenges Phys Chem 89(3):243–245

Lee SHI, Cappato LP, Corassin CH, Cruz AG, Oliveira CAF (2016) Effect of peracetic acid on biofilms formed by *Staphylococcus aureus* and *Listeria monocytogenes* isolated from dairy plants. J Dairy Sci 99(3):2384–2390. https://doi.org/10.3168/jds.2015-10007

Lefevre F, Audic JM, Ferrand F (1992) Peracetic acid disinfection of secondary effluents discharged off coastal seawater. Water Sci Technol 25(12):155–164. https://doi.org/10.2166/wst.1992.0347

Levin DE, Hollstein M, Christman MF, Schwiers EA, Ames BN (1982) A new Salmonella tester strain (TA102) with AXT base pairs at the site of mutation detects oxidative mutagens. Proc Natl Acad Sci 79(23):7445–7449. https://doi.org/10.1073/pnas.79.23.7445

Li Y, Chen DH, Yan J, Chen Y, Mittelstaedt RA, Zhang Y, Biris AS, Heflich RH, Chen T (2012) Genotoxicity of silver nanoparticles evaluated using the Ames test and in vitro micronucleus assay. Mutat Res Gene Toxicol Environ Mutagen 745(1–2):4–10. https://doi.org/10.1016/j.mrgentox.2011.11.010

Li R, Manoli K, Kim J, Feng M, Huang CH, Sharma VK (2021) Peracetic acid-ruthenium (III) oxidation process for the degradation of micropollutants in water. Environ Sci Technol 55(13):9150–9160. https://doi.org/10.1021/acs.est.0c06676

Liberti L, Notarnicola M (1999) Advanced treatment and disinfection for municipal wastewater reuse in agriculture. Water Sci Technol 40(4–5):235–245. https://doi.org/10.1016/S0273-1223(99)00505-3

Luo C, Ma J, Jiang J, Liu Y, Song Y, Yang Y, Guan Y, Wu D (2015) Simulation and comparative study on the oxidation kinetics of atrazine by UV/H_2O_2, UV/HSO_5^- and UV/$S_2O_8^{2-}$. Water Res 80:99–108. https://doi.org/10.1016/j.watres.2015.05.019

Mazhar MA, Khan NA, Ahmed S, Khan AH, Hussain A, Changani F, Yousefi M, Ahmadi S, Vambol V (2020) Chlorination disinfection by-products in municipal drinking water—a review. J Clean Prod 273:123159. https://doi.org/10.1016/j.jclepro.2020.123159

Mezzanotte V, Antonelli M, Azzellino A, Citterio S, Nurizzo C (2003) Secondary effluent disinfection by peracetic acid (PAA): microrganism inactivation and regrowth, preliminary results. Water Sci Technol Water Supply 3(4):269–275. https://doi.org/10.2166/ws.2003.0072

Monarca S, Richardso SD, Feretti D, Grottolo M, Thruston AD Jr, Zani C, Navazio G, Ragazzo P, Zerbini I, Alberti A (2002a) Mutagenicity and disinfection by-products in surface drinking water disinfected with peracetic acid. Environ Toxicol Chem Int J 21(2):309–318. https://doi.org/10.1002/etc.5620210212

Monarca S, Ferett D, Zerbini I, Zani C, Alberti A, Richardson SD, Thruston AD Jr, Ragazzo P, Guzzella L (2002b) Studies on mutagenicity and disinfection by-products in river drinking water disinfected with peracetic acid or sodium hypochlorite. Water Sci Technol Water Supply 2(3):199–204. https://doi.org/10.2166/ws.2002.0103

Mortelmans K, Zeiger E (2000) The Ames Salmonella/microsome mutagenicity assay. Mutat Res-Fund Mol 455(1–2):29–60. https://doi.org/10.1016/S0027-5107(00)00064-6

Muleja AA, Mamba BB (2018) Development of calcined catalytic membrane for potential photodegradation of Congo red in aqueous solution. J Environ Chem Eng 6(4):4850–4863. https://doi.org/10.1016/j.jece.2018.07.004

Neafsey K, Zeng X, Lemley AT (2010) Degradation of sulfonamides in aqueous solution by membrane anodic Fenton treatment. J Agric Food Chem 58(2):1068–1076. https://doi.org/10.1021/jf904066a

Ngigi AN, Magu MM, Muendo BM (2020) Occurrence of antibiotics residues in hospital wastewater, wastewater treatment plant, and in surface water in Nairobi County, Kenya. Environ Monit Assess 192(1):1–16. https://doi.org/10.1007/s10661-019-7952-8

Omrania N, Nezamzadeh-Ejhieha A, Alizadehb M (2019) Brief study on the kinetic aspect of photodegradation of sulfasalazine aqueous solution by cuprous oxide/cadmium sulfide nanoparticles. Catalyst 17:24. https://doi.org/10.5004/dwt.2019.24352

Paumelle M, Donnadieu F, Joly M, Besse-Hoggan P, Artigas J (2021) Effects of sulfonamide antibiotics on aquatic microbial community composition and functions. Environ Int 146:106198. https://doi.org/10.1016/j.envint.2020.106198

Pelalak R, Alizadeh R, Ghareshabani E, Heidari Z (2020) Degradation of sulfonamide antibiotics using ozone-based advanced oxidation process: experimental, modeling, transformation mechanism and DFT study. Sci Total Environ 734:139446. https://doi.org/10.1016/j.scitotenv.2020.139446

Qiu Y, Shi HC, He M (2010) Nitrogen and phosphorous removal in municipal wastewater treatment plants in China: a review. Int J Chem Eng. https://doi.org/10.1155/2010/914159

Raich-Montiu J, Folch J, Compañó R, Granados M, Prat MD (2007) Analysis of trace levels of sulfonamides in surface water and soil samples by liquid chromatography-fluorescence. J Chrom A 1172(2):186–193. https://doi.org/10.1016/j.chroma.2007.10.010

Rossi S, Antonelli M, Mezzanotte V, Nurizzo C (2007) Peracetic acid disinfection: a feasible alternative to wastewater chlorination. Water Environ Res 79(4):341–350. https://doi.org/10.2175/106143006X101953

Santhosh C, Malathi A, Daneshvar E, Kollu P, Bhatnagar A (2018) Photocatalytic degradation of toxic aquatic pollutants by novel magnetic 3D-TiO_2@ HPGA nanocomposite. Sci Reports 8(1):1–15. https://doi.org/10.1038/s41598-018-33818-9

Shafaee M, Goharshadi EK, Mashreghi M, Sadeghinia M (2018) TiO_2 nanoparticles and TiO_2@ graphene quantum dots nancomposites as effective visible/solar light photocatalysts. J Photochem Photobiol a: Chem 357:90–102. https://doi.org/10.1016/j.jphotochem.2018.02.019

Shi XT, Liu YZ, Tang YQ, Feng L, Zhang LQ (2018) Kinetics and pathways of Bezafibrate degradation in UV/chlorine process. Environ Sci Pollut Res 25(1):672–682. https://doi.org/10.1007/s11356-017-0461-9

Snyder SA, Adham S, Redding AM, Cannon FS, DeCarolis J, Oppenheimer J, Wert EC, Yoon Y (2007) Role of membranes and activated carbon in the removal of endocrine disruptors and pharmaceuticals. Desalination 202(1–3):156–181. https://doi.org/10.1016/j.desal.2005.12.052

Sonune A, Ghate R (2004) Developments in wastewater treatment methods. Desalination 167:55–63. https://doi.org/10.1016/j.desal.2004.06.113

Tshangana CS, Muleja AA, Mamba BB (2021) Photocatalytic activity of graphene oxide quantum dots in an effluent from a South African wastewater treatment plant. J Nano Res 24(2):1–15. https://doi.org/10.1007/s11051-022-05422-6

Tshangana CS, Muleja AA, Kuvarega AT, Mamba BB (2022) The synergistic effect of peracetic acid activated by graphene oxide quantum dots in the inactivation of *E. coli* and organic dye removal with LED reactor light. J Environ Sci Health A. https://doi.org/10.1080/10934529.2022.2056385

Wang J, Chu L, Wojnárovits L, Takács E (2020) Occurrence and fate of antibiotics, antibiotic resistant genes (ARGs) and antibiotic resistant bacteria (ARB) in municipal wastewater treatment plant: an overview. Sci Total Environ 744:40997. https://doi.org/10.1016/j.scitotenv.2020.140997

Wu M, Que C, Tang L, Xu H, Xiang J, Wang J, Shi W, Xu G (2016) Distribution, fate, and risk assessment of antibiotics in five wastewater treatment plants in Shanghai, China. Environ Sci Pollut Res 23(18):18055–18063. https://doi.org/10.1007/s11356-016-6946-0

Wu CH, Kuo CY, Dong CD, Chen CW, Lin YL (2019) Removal of sulfonamides from wastewater in the UV/TiO_2 system: effects of pH and salinity on photodegradation and mineralization. Water Sci Technol 79(2):349–355. https://doi.org/10.2166/wst.2019.053

Yan X, Chen H, Lin T, Chen W, Xu H, Tao H (2022) UV/Chlorination of sulfamethazine (SMZ) and other prescription drugs: kinetics, transformation products and insights into the combined toxicological assessment. Environ Technol 43(3):411–423. https://doi.org/10.1080/09593330.2020.1791969

Zhang L, Liu Y, Fu Y (2020) Degradation kinetics and mechanism of diclofenac by UV/peracetic acid. RSC Adv 10(17):9907–9916. https://doi.org/10.1039/D0RA00363H